A04 Reflection of the Earth's surface

Supervisor Name: Dr. Daniel Peters
Candidate number: 32884

26^{th} April 2007

Contents

1 Abstract

The importance of surface albedo measurements is outlined, along with the need for an understanding of the Bidirectional Reflectance Distribution Function (BRDF). A description of albedo and BRDF are given, along with the difficulties in obtaining them. The capabilities of some recent remote sensing instruments are then summarised, with the strengths and weaknesses of each being highlighted. Advancements such as higher resolving power, and improved cloud determination abilities would help future instruments further surface albedo understanding. In addition to this, to reduce costs, more micro-satellites are required. These satellites utilise existing technologies, but can be manufactured for a smaller initial investment. A greater number of sensors, even with current data acquisition abilities would increase the frequency of albedo measurements, and reduce the uncertainties.

2 Introduction

The topic of Earth's climate change has become one of considerable interest in recent years. Both scientists and the media alike have enjoyed persuing answers concerning climate change and its implications to Earth's inhabitants. This recent trend is not about to stop now; increased media coverage, growing awareness, and greater economic impacts are making climate science difficult to avoid. As opposed to just several years ago, few people would deny the importance of understanding our climate, and the impact of any changes to it.

Climate and weather are complex systems, dependent among other factors, on topography, location and the incident radiation from the Sun. A key factor to understanding both weather and climate is understanding the Earth's radiation budget, one critical parameter of which is surface albedo.

Substantial effort has gone into the study of the con-

nections between climate and surface albedo variations. Perusal of General Circulation Model (GCM) studies concerning the climate's sensitivity to desertification [see Xue and Shukla, 1993 [1]] and tropical deforestation [see Hahmann and Dickinson, 1997 [2]] shows a focus primarily on relations between climate response and surface albedo changes. For example, many GCM studies have found that high albedos are closely related to changes in convection and precipitation around rivers, [Charney et al., 1977 [3]; Dickinson and Hanson, 1984 [4]]. Aside from GCM models, extensive research had been carried out using data from satellite observations. These studies can be used to confirm and improve hypothesised correlations between albedo and various climate variables such as land cover type[1]; soil moisture content; cloud cover, and many more besides [see Lucht et al., 2000 [5]]. An example of the effects demonstrated using these models can be seen in work by Kaicun et al., 2004 [6].

This paper will first give some backround details on albedo and the Bidirectional Reflection Distribution Function (BRDF), with an overview on how the two are calculated, and the accuracies required in order for them to be of use in climate models. Following this will be a description of several space-based remote sensing[2] instruments used in albedo determination, detailing their merits and problems. Finally there will be a discussion on the best methods for calculating albedo and suggestions of improvements to current models.

3 Albedo and Bidirectional Reflection Distribution Function

3.1 Albedo

Albedo may be defined as the ratio of the integrated total of reflected solar radiation to the integral of the incoming solar radiation [Monteith, 1973 [7]]. The overall solar radiation absorbed by the ground at the Earth's surface is directly affected by the land surface albedo. As a consequence, the climate responds to changes in albedo; both induced by natural causes, and anthropogenic. Theoretically, albedo can range from zero, (a black surface that absorbs all incident radiation), to unity, (a surface that reflects all incident radiation).

Current methods for obtaining surface albedo are split into two main categories. There are remotely sensed and in situ methods[3]. In this paper, details on the remotely sensed satellite instruments will be explained, and how the sensors have developed over the years.

In situ albedo determinations often use land cover-type maps to differentiate between the main surface cover types. An average albedo value is then applied to each surface type. However, without a detailed knowledge of the surface, this method incurs problems. The trouble can be seen by examining the areas covered by snow, in which the uncertainties are particularly large. For example, if an albedo value of 0.75 is applied to snow covered areas, uncertainties of up to 50% are often observed, and uncertainties can be as high as 75% [Maurer, 2002 [8]]. This is because snow albedo is a highly varying quantity. For melting snow, the albedo might be 0.4, whilst for fresh snow, the albedo may be as high as 0.9. In the other extreme, muddy snow can have an even lower albedo of around 0.2. So without the ability to differentiate between types of snow, the albedo data in snow covered areas are of limited use. Similar problems in albedo determination by this method are seen with other land types. In contrast, measurements via remote sensing can return albedo estimates with smaller uncertainties than those based purely on land type as they use an alternative method. Satellites are used to infer surface albedo from the radiation leaving a given area. Sellers et al., 1993 [9] and Liang et al., 2003 [10] stipulated that albedo accuracies of around ± 0.2 are necessary for modelling of surface albedo and the Earth's surface energy budget. These requirements are now being achieved by remote sensing instruments, and the results are sufficiently accurate to improve GCMs.

3.2 Bidirectional Reflectance Distribution Function

Unlike simple theoretical models, Earth's surface does not reflect isotropically. When deriving the surface albedo, this anisotropic surface reflectance needs to be taken into account, for which knowledge of the Bidirectional Reflection Distribution Function (BRDF) is required. The BRDF is a function at a given surface - not at the top of the atmosphere. However, satellites measure radiation from space, and so utilise BRDF

[1] See Appendix A for explanation of Land Cover Type.

[2] Remote sensing covers all measurements that are not in situ (See Appendix A). This includes both field-based and satellite-based measurements. In this paper, only instruments aboard satellites will be considered. From here on, remote sensing refers only to satellite-based remote sensing.

[3] See Appendix A for explanation of In situ.

models based on radiative transfer theory, using surface topography, aerosol size and type, and the optical thickness of the atmosphere to provide an approximate BRDF for the surface being viewed [Stroeve et al., 1997 [11]].

The Bidirectional Reflectivity, (Figure 1) is defined to be the reflected radiance divided by the incident irradiance [Nicodemus, 1965 [12]]. The BRDF is then defined as how the bidirectional reflectivity varies with angle,

$$BRDF = \frac{L_r(\theta_i,\phi_i\theta_r,\phi_r,\lambda)}{E_i(\theta_i,\phi_i,\lambda)}$$

Where θ is the zenith angle[4] and ϕ is the azimuth angle[5], (as shown in Figure 2). The subscripts i and r represent incident and reflected radiation respectively (see Figure 1) and λ represents the wavelength. The above definition of BRDF has units of steradians^{-1}.

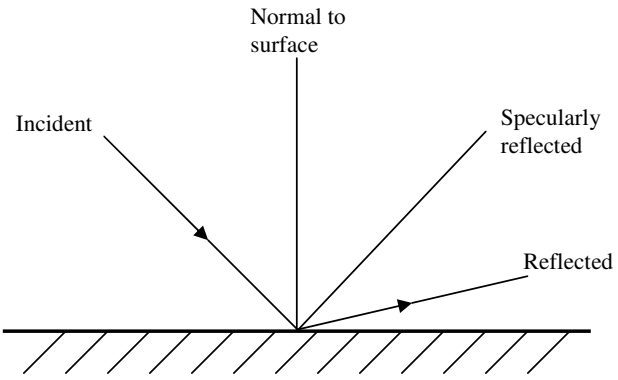

Figure 1: Bidirectional Reflectivity: reflected radiance divided by incident radiance.

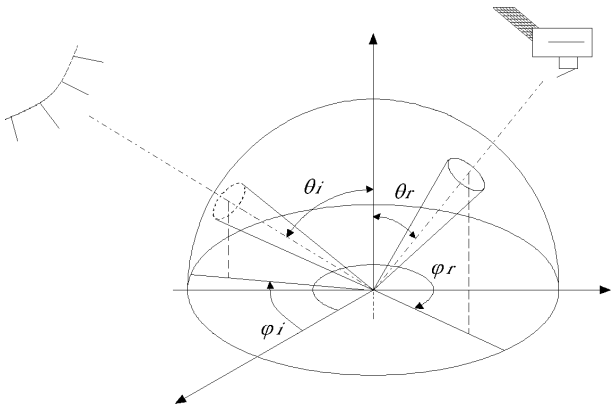

Figure 2: BRDF convention for angles. θ_i is the zenith angle and ϕ_i is the azimuth angle. The subscripts i and r represent incident and reflected respectively, and λ is the wavelength.

[4]See Appendix A for explanation of Zenith Angle.

[5]See Appendix A for explanation of Azimuth Angle.

The BRDF should, in thoery, be unitless, as it is fundamentally a reflectance (a ratio). However, in practice, measurements can only be taken over a finite solid angle, and so the measured BRDF is dependent on this solid angle.

It should be noted at this point that some models, (not included in this paper) avoid the complications of BRDFs, by assuming a purely Lambertian surface[6]. This greatly simplifies the problem, as the BRDF is simply a constant for a Lambertian surface, as the surface has equal incident and exitant radiation at all viewing angles. However, purely Lambertian-based models have been shown to yield less accurate results for albedo than models which take BRDF into account [Ni and Li, 2000 [13], Vermote et al., 1997 [14]]. In addition to this, increased turbidity of the atmosphere further increases the uncertainties in models that do not consider the BRDF [Wanner et al., 1997 [15]].

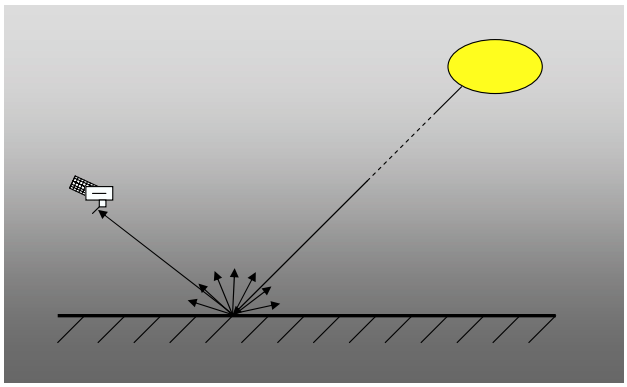

Figure 3: BRDF of Lambertion surface- equal radiance in all directions e.g. a cinema screen.

Since no natural surfaces are Lambertian, deducing the BRDF becomes a complex problem in anything other than a theoretical context. Obviously, it is impossible to measure an infinite number of reflectances for a given point (one reflectance per infitessimal solid angle), so the BRDF must be estimated. Combined with the fact that the BRDF is wavelength dependent, it is easy to see how the BRDF is a limiting factor in deriving the surface albedo. For example, depending on the view angle, and the illumination angle, a surface may result in overall forward scattering (Figure 4) or backward scattering of radiation (Figure 5) [Brown de Colstoun et al., 1996 [16]]. As sensors only view at a few angles, something as simple as this becomes an issue in BRDF determination.

In summary, the BRDF, is affected by many physical factors, such as surface cover type, atmospheric

[6]See Figure 3 and Appendix A for explanation of a Lambertian surface.

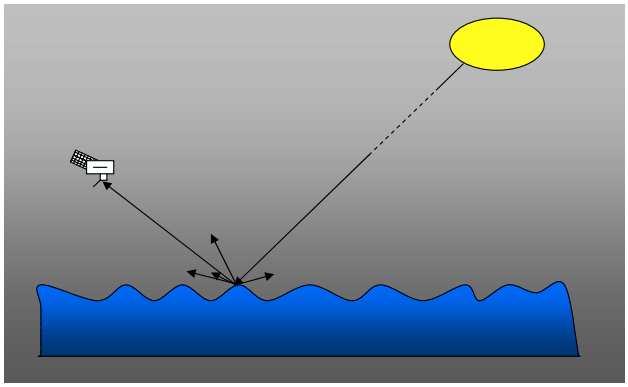

Figure 4: Example BRDF for overall forward scattering surface.

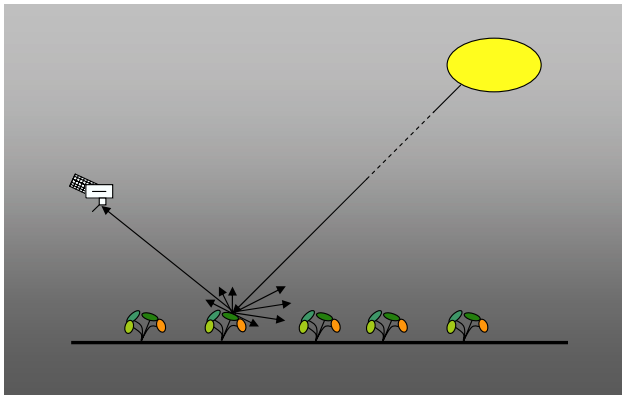

Figure 5: Example BRDF for overall backward scattering surface.

conditions, and ground conditions. Remote sensing from satellites provides the best way of obtaining accurate global coverage of the BRDF. An improved understanding of the BRDF and how physical factors affect it is paramount for advancement in global surface albedo measurements and climate prediction.

4 Remote Sensing Instruments

For obtaining both local and global surface albedo values, satellite remote sensing, with their frequent repeat global coverage, offer the best current solution. However, far from being the end of the story, many complications arise in measuring surface albedo from satellites.

Remote sensing instruments infer surface albedo from measurements by processing the radiance measurements obtained from the top of the atmosphere. In order to return a result, cloud-covered and cloud-free pixels are first distinguished, with cloud covered pixels ignored for the calculation of surface albedo. Next, the digital data is calibrated to represent radiance [Sutherland et al., 1997 [17]]. An atmospheric correction is then applied to the data before surface reflectance is obtained by dividing the data by the Planck irradiance function. The result is then transformed from narrow band data to wider band data, in order to be compatible with existing climate models.

There are four main sources of uncertainties in the method used by remote sensing instruments. Satellites can often have trouble distinguishing between snow-covered and cloud-covered areas. This results in some snow-covered pixels being ignored, and some cloud-covered areas being considered as snow-covered. More uncertainties are incurred when measurements are adjusted to take into account atmospheric corrections in absorption and scattering, as these corrections are complex and difficult to compute. Furthermore, measurements are often made over narrow spectral bands, and need to be converted to wider bands in order to be useful with climate models. In addition, the data are dependent on viewing and illumination angles, and so the BRDF must be taken into account. Due to these limitations, remotely sensed data is compared with albedos derived historically [Wei et al., 2001 [18]].

As discussed above, remote sensing instruments do not measure surface albedo directly. Instead, the BRDF, and consequently, the albedo, is estimated. The instruments use reflectance data along with models of how the surface scatters radiation at various angles of inclination and viewing. Three important parameters must be taken into account when assessing a remote sensing instrument's adeptness at deriving BRDF and albedo [Barnsley et al., 1994 [19]].

1. The angular range over which the instrument obtains results.

2. The time period the instrument records data over.

3. The ground latitude and orbit of the satellite that the instrument is placed on.

Possibly the most important of these is the instrument's angular range.

The sensors mentioned make recordings of the radiation reflected from the Earth's surface, not the incident radiation. In order to gain an accurate estimate of the BRDF, the angle of the solar illumination is an important influence to take in to account. It will vary considerably during a year due to the season, and significant daily fluctuations also occur. Ground latitude and the positioning of repeat cycle orbits also affect data. The degree to which data from different times contribute to BRDF samples will depend not only on

atmospheric conditions, but also on the state of the ground surface. For example, in the short-term, the moisture content of soil can change rapidly during a sudden downpour of rain. Longer-term, the hydrosphere[7] cycles result in varying soil moisture composition. Furthermore, remembering that atmospheric conditions will be changing on a daily basis, it is not surprising that more primitive remote sensing instruments (with their longer acquisition times) aim to weigh up the angular spread and the number of measurements with the time period over which they are obtained. Unfortunately, the result is that these sensors produce rather sparse sampling of BRDF. More modern instruments with greater computing power, higher resolution sensors, and knowledge gained from earlier surface albedo projects provide denser, more accurate sampling.

4.1 HRS/HRG, ETM+, ATSR, AVHRR and ALI

4.1.1 HRS and HRG

The Système Pour l'Observation de la Terre 5 (SPOT 5) is a continuation of the SPOT 1 to 4 satellites that preceded it. The earlier satellites gained a reputation for reliable data acquisition, and the new incarnation builds on this base. The new High Resolution Stereoscopic (HRS) sensor improves resolution over SPOT 4 from 20m to 10m in the multispectral range, whilst the High Resolution Geometric (HRG) sensor obtains resolutions of 5m (as opposed to 10m from SPOT 4). In 'Supermode', resolutions of as high as 2.5m are possible [Larty and Rouge, 2002 [20]]. The HRS cameras can scan forward and aft at angles of up to 20°, and the HRG cameras also use an along-track scanning technique to scan at angles of up to 27°. In addition to the HRS and HRG instruments, SPOT 5 carries two other instruments. VEGETATION 2, measures vegetation cover on a daily basis, and Doppler Orbitography and Radiopositioning Integrated by Satellite (DORIS) helps to determine the exact location of the satellite at any time [Barre et al., 2003 [21]]. Together, SPOT's instruments build an accurate three dimensional map of the Earth's surface every twenty six day cycle. These maps, along with BRDF data return albedo values every cycle. The maps are useful for returning albedo values on a global scale, but the BRDF sampling is too sparse, and the cycle time is too long relative to other data available from more advanced sensors.

[7] See Appendix A for explanation of Hydrosphere.

4.1.2 Enhanced Thematic Mapper Plus

The Landsat Enhanced Thematic Mapper Plus (ETM+) is a modification to the popular Landsat Thematic Mapper (TM) instrument, used on earlier Landsat projects. The Landsat program is the longest continuous record of Earth's surfaces, with Landsat 1 launched in 1972. The ETM+, which is aboard Landsat 7, takes 16 days to completely cover the Earth's surface, although some areas, (for example, high latitude regions) are measured more than once in this time. This results in denser BRDF sampling, and therefore more accurate albedo values in these areas. The ETM+ boasts spatial resolutions of 15-60m (depending on the spectral band), using a fixed multispectral radiometer [Landsat website [22]], and a fairly narrow 183km swath[8]. The TM had a fixed viewing angle of 11°, seriously limiting its ability to explore the surface BRDF [Barnsley et al., 1994 [19]]. Despite this, data obtained by TM does show angular variations of reflectance. Unfortunately, unless at particularly high altitudes, TM's ability to use seasonal variations in angular reflectance to improve BRDF sampling was limited by the (fixed) equator crossing time of its orbit. The ETM+ also uses a nadir[9] viewing sensor, but provides much improved BRDF sampling [National Aeronautics and Space Administration (NASA) Landsat website [23]]. However, the instrument suffers from its narrow swath width. Being only 183km means the ETM+ takes 16 days to view the whole of the Earth's surface.

4.1.3 Advanced Land Imager

In late 2000, the Advanced Land Imager (ALI) was launched. Its purpose was for validation of ETM+ data, and development of cost-saving methods that could be applied to the next generation Landsat. ALI can achieve impressive resolutions of up to 10m. Although only minor improvements were made to the performance of ALI compared to ETM+, it was made considerably cheaper, smaller and lighter. Future Landsat missions will benefit from the technologies used, and costs should be reduced by a factor of at least four [Earth Observing website [24]].

[8] See Appendix A for explanation of Swath.

[9] See Appendix A for explanation of Nadir.

Table 1: Details of the HRS/HRG, ETM+, AATSR, AVHRR and ALI instruments. In the 'Scanning type' row, Cross-track and Along-track are abbreviated to Cross-T and Along-T respectively. For an explanation of the terms Along-track and Across-track/Cross-track, see Appendix A.

Sensor	HRS/HRG	ETM+	ALI	AATSR	AVHRR
Satellite	SPOT 5	Landsat 7	EO-1	Envisat	NOAA-18
Year of Launch	2002	1999	2000	2002	2005
Spatial resolution	2.5-10m	15-60m	10-30m	1km	1.1km
Orbital altitude /km	822	705	705	790	833
Orbital inclination /°	98.7	98.2	98.2	98.55	98.7
Orbital period /s	6106	5930	5930	6035	6120
Equatorial cross-time	10:30	10:05	10:30	10:00	13:30
Number of orbits per cycle	369	233	233	501	28.3
Time for global coverage /days	26	16	16	35	2
Swath width /km	120	183	37	256	2400
Number of spectral bands	5	8	10	7	6
Spectral range /μm	0.48-1.75	0.45-12.5	0.43-2.35	0.5-12.0	0.58-12.5
Viewing angles along-track /°	$\pm$20.0, $\pm$27.0	n/a	n/a	0-55	n/a
Viewing angles across-track /°	n/a	n/a	15.0	n/a	-54.0 - +54.0
Scanning type	Along-T	n/a	n/a	Conical	Cross-T

4.1.4 Advanced Along-Track Scanning Radiometer

The Advanced Along-Track Scanning Radiometer (AATSR) takes a different approach to most sensors. It uses a forward-facing conical scan[10] to give two views of a 256km swath per orbit. At a given point, it performs a scan almost at nadir, followed by a sweeping conical scan. The forward pointing scan includes a view along the ground-orbit, ahead of the AATSR up to an angle of 55° from nadir [AATSR webstie [25], see Figure 6 in Appendix A]. When the satellite passes over this previously forward-viewed point, another near-nadir scan is taken. Comparison of the two views of the same point on the ground allows AATSR to calculate atmospheric corrections. These atmospheric corrections can be up to 20% more accurate than those obtained by multi-channel sensors [AATSR website [25]]. As a result of rigorous testing and calibration, AATSR is capable of highly precise measurements. However, it concentrates on measuring the sea surface temperature, and so is of limited use regarding localised land surface albedo. Where it is of use is determination of global and oceanic energy balances, which in turn can be used to help derive global albedo. Despite its lack of direct contribution of BRDF data products, AATSR's technological advancements will be used on future sensors to acquire higher accuracy BRDF data [Prata, 2002 [26]].

[10] See Appendix A for an explanation of AATSR's Conical Scan.

4.1.5 Advanced Very High Resolution Radiometer

The Advanced Very High Resolution Radiometer (AVHRR) is one of the older albedo measurement instruments, but still an important one. It was first launched aboard the TIROS-N in 1978, and has been improved to the current 6-channel (three visible and three infrared) version aboard the National Oceanic and Atmospheric Agency's eighteenth satellite (NOAA-18), launched in 2005. It has 1.1km spatial resolution at nadir, measuring one view over various wavelengths, covering infrared, near-infrared, and visible regions.

The AVHRR has an advantage of being able to minimise the problem of differentiating between snow and clouds by covering the Earth many times, and thus reducing uncertainties incurred. The AVHRR has proved useful for validating newer models such as those used by the MODerate Resolution Imaging Spectroradiometer (MODIS); the Algorithm for MODIS Bidirectional Reflectance Anisotropy of the

Land Surface (Ambrals) BRDF model discussed below. The AVHRR's data is good enough for an approximate fit to the actual values of surface albedo, but does have room for improvement. Running models such as the Ambrals BRDF on older AVHRR data, and comparing their results to more accurate data now available, has proved to be a useful method of testing the new models [Strugnell and Lucht, 2001 [27]; Csiszar and Gutman, 1999 [28]].

Although the AVHRR is able to take readings from view zenith angles of up to 54°, it is only because it has a wide field of view, not because the sensors are moveable or stationed at an array of angles. The result is that by modern standards, it only gives relatively sparse BRDF sampling -at the equator, as few as five different viewing angles are observed per crossing (although this number will increase with latitude) [Greuell and Oerlemans, 2005 [29]]. However, due to AVHRR's low cost, and spatial characteristics, it is well suited to monitoring the annual and seasonal changes in the surface land cover.

4.2 POLDER, ASTER, MISR and MODIS

Despite being used for various BRDF models, the instruments discussed so far are not optimised for BRDF determination. The following sensors were all developed specifically for BRDF acquisition.

4.2.1 POLDER

The POLarazation and Directionality of the Earth's Reflectance (POLDER) was first launched in 1996, and makes use of a two dimensional Charge-Coupled Device (CCD) array, and a wide scanning angle both along-track (86°), and across-track (102°). POLDER 2 was launched late 2002. It uses the same scanning angles with improvements to the POLDER products, and absorption and backscattering coefficients, for water in particular. At the time of launch, this Japanese-French effort was the only satellite instrument capable of giving the polarization, directionality and multispectral signature of detected radiation. Despite the improvements, POLDER 2 is only capable of a resolution of 6km, but can achieve an impressive 3% relative accuracy in BRDF products [Hautecoeur and Roujean, 2007 [30]]. The BRDF and albedos are derived using an adjusted version of the Li-Ross kernel-driven model to gain such high accuracies, (similar to that used in the Ambrals model - see section 5).

Often, remote sensing instruments that derive surface BRDF suffer a reduction in the sampling density of their results near the poles due to increased cloud cover at higher latitudes. An advantage of POLDER 2 over other remote sensing instruments is that it returns results with increasing frequency at increasingly higher latitudes, due to its orbit. This orbital characteristic dramatically improves BRDF sampling at higher latitudes, [Hautecoeur and Roujean, 2007 [30]].

4.2.2 ASTER

The Advanced Spaceborne Thermal Emission and Reflection Radiometer (ASTER) was launched aboard the Terra satellite as part of NASA's Earth Observing System (EOS) program late in 1999. It is an imaging radiometer, which obtains data at nadir views in 14 spectral channels. Using a swath of 60km, and an oscillating mirror to view up to 8.55°, (near infrared and infrared) and 24°, (visible and near infrared) across-track and 27° along track, ASTER is able to view the whole of the Earth's surface every sixteen days [NASA, 1990 [31]]. ASTER is capable of high spatial resolutions (15 - 90m, depending on the spectral band), and so is used for calibration and validation of the other instruments aboard the Terra satellite, along with land surface studies of its own (in particular, surface height mapping). It allows users to zoom in on areas of interest, or uncertainties flagged up by other sensors with inferior resolution. ASTER uses a simple version of the Multiangle Imaging SpectroRadiometer's (MISR -see Section 4.2.4) fore and aft viewing camera array to view multiple paths along-track. The high spatial resolution of ASTER has proved to be particularly useful in the calibration of BRDF for snow covered areas. In some earlier models, snow covered surfaces are considered to be lambertian. This was acceptable because the uncertainties induced in these areas were still less than the uncertainties from other land cover types. However, as accuracies in BRDF determination have improved, the relative uncertainty from a lambertian approximation for snow has increased. Despite this, ASTER has been used to great effect to calibrate the BRDF for snow covered areas [Tsuchida, 1999 [32]].

4.2.3 MODIS

The MODerate Resolution Imaging Spectroradiometer (MODIS) was designed as an instrument to improve upon the AVHRR, and can be found aboard the Terra and Aqua satellites. Aqua orbits the Earth from south to north, passing over the equator during the afternoon, whilst Terra orbits north to south,

Table 2: Details of the POLDER 2, ASTER, MISR and MODIS instruments. In the 'Scanning type' row, Cross-track and Along-track are abbreviated to Cross-T and Along-T respectively.

Sensor	POLDER 2	ASTER	MODIS		MISR
Satellite	ADEOS 2	Terra	Aqua	Terra	Terra
Year of Launch	2002	1999	2002	1999	1998
Spatial resolution	6km	15-90m	0.25-1km	0.25-1km	0.275-1km
Orbital altitude /km	803	705	705	705	705
Orbital inclination /°	98.7	98.2	98.2	98.2	98.2
Orbital period /s	6056	5930	5930	5930	5930
Equatorial cross-time	10:30	10:30	13:30	10:30	10:30
Number of orbits per cycle	57	233	233	233	233
Time for global coverage /days	n/a	16	1-2	1-2	2-9
Time for one cycle /days	4	16	16	16	16
Swath width /km	2400	60	2330	2330	360
Number of spectral bands	9	14	36	36	4
Spectral range /μm	0.44-0.91	0.5-11.65	0.4-14.4	0.4-14.4	0.4-0.89
Viewing angles along-track /°	-43.0 - +43.0	0.0, -27.6	n/a	n/a	$\pm$70.5, $\pm$60.0, $\pm$45.6, $\pm$26.1, 0.0
Viewing angles across-track /°	-51.0-+51.0 -51.0-+51.0	$\pm$8.55, $\pm$24.0	$\pm$55.0	$\pm$55.0	$\pm$15.0
Scanning type	Cross-T Along-T	Cross-T Along-T	Cross-T	Cross-T	Along-T

passing over the equator in the morning. Between them Aqua MODIS and Terra MODIS view the whole of the Earth's surface, (save for a small area around the equator – see Section 4.2.4), every one-to-two days. The first MODIS program was launched in late 1999 on the Terra satellite, and Aqua MODIS was later launched in 2002 [MODIS website [33]]. MODIS takes sequential cross-track views over multiple angles, gradually building up surface BRDF products over 16 days, [Schaaf et al., 2002 [34]]. MODIS can achieve consistently high spatial resolution of between 250m and 1km at nadir, (the actual resolution of data depends on the band being used). Bi-hemispherical albedo[11] (also known as white-sky albedo); directional-hemispherical albedo (black-sky albedo); Nadir BRDF-Adjusted surface Reflectances (NBAR[12]; model parameters describing the BRDF; and detailed quality information are all incorporated into each product produced by MODIS [Schaaf et al., 2002 [34]]. The quality information allows users to assign weights to each pixel. This gives users the choice between accuracy and sampling density (as the accuracy threshold of BRDF products is improved, the sampling density will decrease). This feature of MODIS data becomes more important when using the Ambrals BRDF products (see Section 5).

4.2.4 MISR

The Multiangle Imaging SpectroRadiometer (MISR) was launched in 1998 as part of NASA's EOS, aboard the Terra satellite along with ASTER and MODIS. MISR's nine cameras image along-track, with four forward facing, four aft looking, and one nadir viewing [MISR website [35]]. Its multi-camera setup gives MISR the advantage of being able to obtain surface BRDF to a high degree of accuracy and frequent global coverage. To allow for a non-lambertian surface without multiple simultaneous views would mean making many passes over the same point – thus increasing the time to acquire data, and making the data susceptible to daily atmospheric changes. Other benefits of the multiple cameras include improved ability to distinguish between similar-looking surface features, and a lack of uncertainties incurred by surfaces with abnormally high reflectances (for example the

[11] See Appendix A for explanations of Bi-hemispherical and Directional hemispherical albedos.

[12] See Appendix A for explanation of NBAR.

glint from an ocean on a clear, sunny day). The nine cameras also drastically improve MISR's ability to deal with clouds. Cirrus clouds, (often hard to detect) are detected at large viewing angles due to the increased optical path of radiation incident on the cameras. For denser clouds, MISR creates a three dimensional representation of the clouds, allowing their height to be derived. MISR uses wavelengths close to MODIS's to take observations in four spectral bands (per view) covering visible and near-infrared. Like MODIS, MISR provides data with a spatial resolution of 1.1km, although in theory it can obtain data with spatial resolutions as high as 275m [Diner et al., 2002 [36]]. MISR takes sequential views over multiple angles, gradually building up surface BRDF over 16 days. MISR uses various photodiodes and diffuser plates, along with various validation programs, (for example the Portable Apparatus for Rapid Acquisition of Bidirectional Observation of the Land and Atmosphere (PARABOLA III)), to acquire a high degree of relative and absolute calibration. MISR proves itself particularly useful in the supplementation of missing MODIS data. As MODIS crosses the equator, some data across the swath are lost due to glint from the ocean. MISR does not suffer from such problems as it scans along track with a narrower swath, and so helps to fill a significant proportion of the missing data lost by MODIS.

A slight drawback of MISR is that it suffers from is a lack of consistency of image size for a given point on the ground. This occurs due to a combination of factors; the cameras, the rotation of the Earth and the satellite's orbit. The nine cameras do not employ the same optical design, so return images with different areas. Adding to this, in the time it takes the cameras to acquire information, (a few minutes) the Earth has rotated. Although the cameras are angled to account for this, it is very rare to find two views from the same orbit with precise overlap. Finally, the satellite's orbit will vary from one orbit to the next, both in position and direction, (an uncertainty of up to a 20km is expected) [Diner et al., 2004 [37]]. These three factors all contribute to MISR's inconsistent image size.

5 Ambrals BRDF/Albedo Product

The Algorithm for MODIS Bidirectional Reflectance Anisotropy of the Land Surface (Ambrals) uses multispectral data and a semi-empirical kernel-driven model to build a mosaic of 1x1km pixels. It relies on the weighted sum of an isotropic parameter and two functions (otherwise known as kernels) of viewing and illumination geometry to determine reflectance. It uses kernel functions in five forms, enabling it to characterise surface, volume and isotropic scattering [Zhang et al., 1995 [38]]. So as to avoid limiting the algorithm, a spatial resolution of 1km is used for each pixel, (using MODIS's highest possible resolution of 250m would reduce the number of pixels available for use). Albedo and BRDF products are acquired in seven spectral bands every 16 days for each pixel [Running et al., 1994 [39]]. In addition to directional (black-sky) and diffuse (white-sky) albedos, the products give a full global surface BRDF. Furthermore, pixels are assigned quality flags giving, amongst other data, the Root Mean Square Error (RMSE), allowing the user to allocate weightings to each. The MODIS BRDF/albedo product has a far higher spatial resolution than data available before its development. The International Satellite Land Surface Climatology Project (ISLSCP) had a resolution of 1° x 1°, and the Earth Radiation Budget Experiment (ERBE) had a resolution of 2.5° x 2.5°[Wanner et al. 1997 [15]], whilst the MODIS BRDF/albedo product has a quarter-degree resolution. The superior resolution results in two main advantages; improved determination of any small fluctuations; and closer matching of albedos with land cover types. Overall, the kernel-drivel model has been demonstrated to work consistently well, on application to field- and laboratory-measured reflectance data [Disney et al., 2004 [40]].

5.1 Suitability of Ambrals Model

The Ambrals BRDF model benefits from the advantages of both empirical and physical models, and so is chosen above others to derive albedo. The top-down method employed by the Ambrals model ensures immediate advantages over other BRDF models; it does not assume homogeneous land cover types for a given pixel; it can show how uneven topography affects BRDF; and it it secure against noisy input data and limited angular sampling [Chen et al., 1999 [41]]. Also, the Ambrals model uses just three parameters, eliminating the need for external inputs. In addition to this, being reflectance-based, there is no need to use pre-determined databases of vegetation properties [Privette and Vermote, 1995 [42]]. These databases often have poor spatial resolution compared to the 1km resolution of the MISR and MODIS instruments, and avoiding them retains the quality of BRDF

products. Furthermore, the Ambrals model boasts a fast inversion of data into BRDF/albedos, making it ideal for BRDF inversion on a global scale operation. The final advantage of the Ambrals model is that it can be scaled [Wanner et al., 1997 [15]], allowing it to be applied to data with inferior resolution, and thus increasing its potential uses.

The kernels are derived from volume scattering radiative transfer models [Ross, 1981 [43]], and from surface scattering geometric shadow casting theory [Li and Strahler, 1992 [44]]. Among others, studies such as Privette, Eck and Deering, 1997 [45] and Wanner, Li and Strahler, 1995 [46], have shown RossThickLiSparse-Reciprocal kernel combination to be most suited to the MODIS algorithm. The model samples from a large remotely sensed database of directional reflectances to characterise the BRDF, resulting in consistently reliable surface albedos and surface reflectances for a wide range of surface cover types, [Wanner et al., 1997 [15]]. They are fairly insensitive to noisy data [Lucht and Lewis, 2000 [47]], and return reliable results even when presented with a small amount of input data [Lucht, 1998 [48]].

Extensive validation of the Ambrals model has been carried out by numerous studies using existing data. Privette and Vermote, 1995 [42] showed the Ambrals model to perform good corrections to AVHRR desert data. Li et al., 1996 [49] successfully removed overlapping image borders on AVHRR Normalised Difference Vegetation Index (NDVI). Wu et al., 1995 [50] derived accurate BRDF products from AVHRR for various land cover types, and d'Entremont et al., 1996 [51] carried out successful studies on AVHRR inversions. Advanced Solid-state Array Spectroradiometer (ASAS) data and the Walthall model have also demonstrated the abilities of the Ambrals BRDF model -proving its ability to return consistently accurate albedo data even at wide viewing angles, [Strahler et al., 1995 [52], Liang et al., 1997 [53] and Barnsley et al., 1997 [54]]. Further assurance of the Ambrals model comes from BOReal Ecosystems Atmosphere Study (BOREAS) data that successfully acquired accurate savanna woodland albedos [Deering et al., 1995 [55]]. Post launch validation has also been carried out with agreeable results by Flynn et al., 1997 [56], Stroeve et al., 2005 [57] and Kaicun et al., 2004 [6] to name but a few.

6 Conclusions

Detailed knowledge of the BRDF is critical to understanding the ongoing and potential future changes to Earth's climate. The remote sensing instruments discussed allow surface albedo estimates to be obtained faster and more accurately than ever before. However, for our understanding of surface albedo to to progress, advancements in models, and instruments must continue.

Semi-empirical models should be improved upon further. The Ambrals RossThick-LiSparse BRDF model has been shown to be a particularly suitable basis for further advancements. Great possibilities exist if models are adapted to make accurate use of information from sensors that have not previously been used. For example, the Okean-O is a Russian satellite that has sensors on board that are capable of resolutions of 50m, but is used solely for monitoring the oceans. Similarly, QuickBird-2 obtains images with a 0.5m resolution, but is used mainly for rural and urban planning, and mapping. If data from existing sensors such as these could be used in BRDF models, the need for large expenditure on many new satellites would be reduced. Hundreds of satellites are planned for launch in the next few years -using the information they gain in BRDF models would further surface albedo understanding dramatically.

Even with improved modelling methods, there would still be a need for more instruments that are optimised for BRDF determination. There is much to be gained from small, cheap satellites, utilising current technologies. More satellites with instruments similar to MISR and MODIS would increase the frequency of global coverage and reduce error rates for a lower cost than developing completely new satellites. There would of course still be a need for advancing the abilities of sensors. One major area requiring improvement is cloud determination methods. The main cause of problem are thin, cirrus clouds, as they often go undetected by sensors, despite affecting albedo values. In addition, there is a need to hone sensors' abilities to differentiate between snow or ice covered ground, and ground below clouds. Often pixels are discarded by sensors that believe snow covered ground is simply clouds hiding the ground below.

Another area in need of improvement is instruments' resolution. Further improvements to the resolving power of sensors would mean smaller pixels, and therefore more accurate albedo data.

To improve both instruments and models, consider-

able funding is required. Highlighting the commercial benefits, (such as improved weather prediction, more frequent weather forecasts etc.) to companies could significantly help with funding. Many satellites are planned for launch within the next few years. They should improve upon the existing instruments, and help further our understanding of the Earth's atmosphere. The HYDROsphere State (HYDROS) mission should be launched in 2009. It will be the first satellite capable of mapping the moisture content of the Earth's surface, and is hoped to greatly increase our knowledge of the energy balance at the Earth's surface. The National Polar-orbiting Operational Environmental Satellite System (NPOESS) should return measurements on many of the parameters affecting climate change, as well as having an increased accuracy and frequency of albedo retrieval.

Current instruments will continue to reinforce our knowledge of surface albedo, and development of future sensors will further advance our understanding of climate systems as a whole. BRDF and albedo determination is an important subject, not only for the scientists involved, but for the world community as a whole. Appropriately, funding is set to continue.

A Explanations

AATSR conical scanning (see Figure 6).

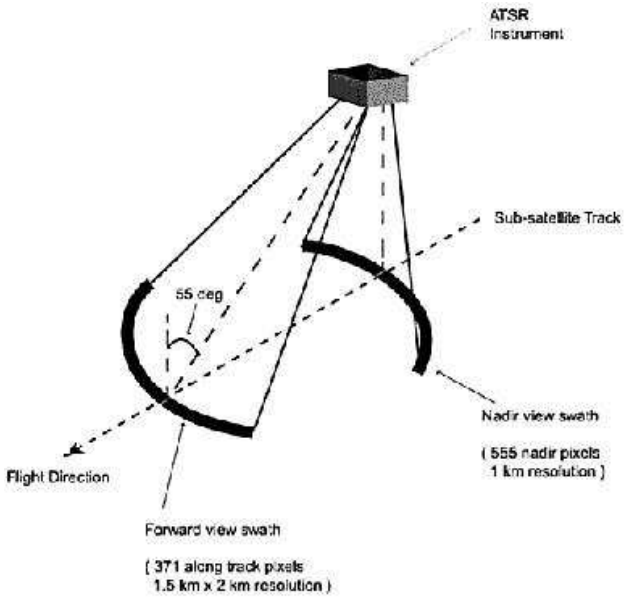

Figure 6: ATSR/AATSR conical scanning.

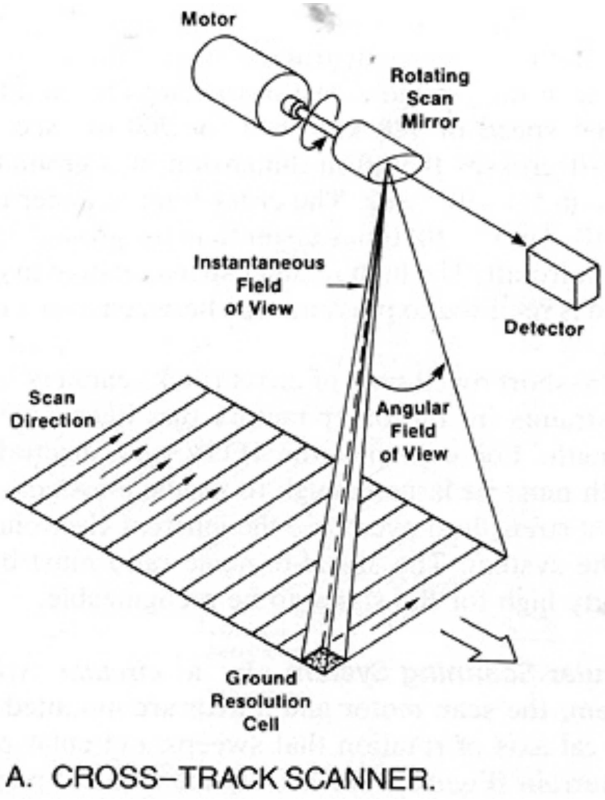

Figure 7: Cross-track scanner. From Sabins, 1979 [58].

Across-track/Cross-Track: Refers to the direction perpendicular to the track (See 'Track'), (i.e. perpendicular to the direction of the satellite). See Figure 7.

Across-track Scanner: An Across-track scanner, (See Figure 7) usually makes use of an oscillating (or rotating) mirror to view across-track. The distance across-track is of the order of kilometers, whilst the depth is of the order of metres. The method of viewing across-track is also referred to as whiskbroom scanning. Only one element is required to be calibrated.

Along-track: Refers to the direction parallel to the track (See 'Track'), (i.e. parallel to the direction of the satellite). See Figure 8.

Along-track scanner: An Along-track scanner, (See Figure 8) usually uses an array of detectors, lined up to view along the direction of the track. Each detector (usually a CCD) corresponds to one pixel. The method of viewing along-track is also referred to as pushbroom scanning. In contrast to across-track scanning, along-track scanning requires that each element is calibrated.

Azimuth: The angle measured clockwise from a base point (often North) to the point directly below the observed object. The horizon is defined as a circle centred on the observer, that is horizontal with respect to the observer.

Bi-Hemispherical Reflectance: (White Sky Albedo) is defined as the reflectance of a surface subject to diffuse illumination, (i.e. no direct component). It is the integral of BRDF over all viewing and illumination angles of the hemisphere in consideration.

Black Sky Albedo: See Directional Hemispherical Reflectance.

Directional Hemispherical Reflectance: (Black Sky Albedo) is defined as the reflectance of a surface subject to direct illumination, (i.e. no diffuse component). It is the integral of BRDF over all viewing angles.

Hydrosphere: All of the Earth's water- in solid, liquid and gaseous forms. It includes any water inside the outer atmosphere; oceans, clouds, glaciers etc. [Poehls and Smith, 2007 [59]].

In situ: In an atmospheric context, in situ describes instruments taken in direct contact with the object being measured.

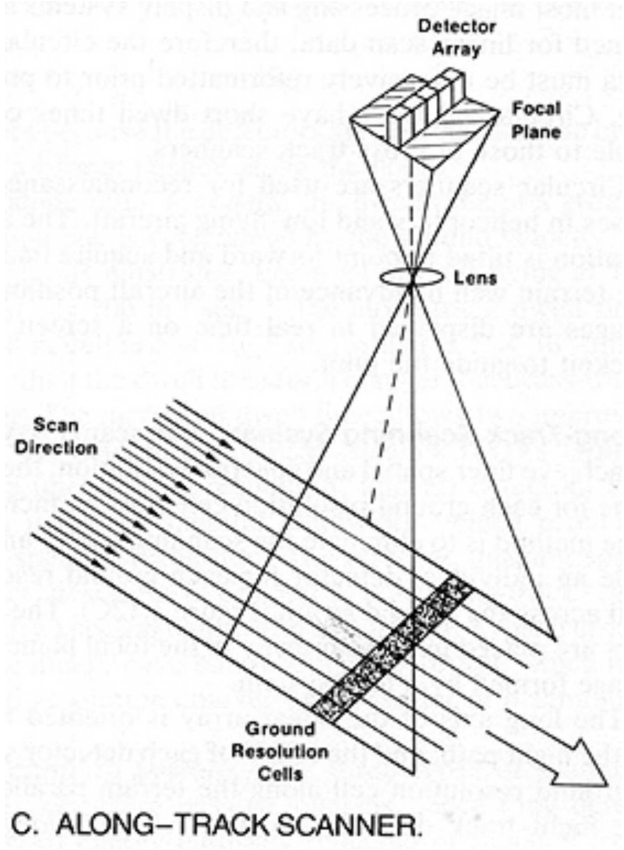

Figure 8: Along-track scanner. From Sabins, 1979 [58].

Lambertian surface: A surface that has a constant radiance that is independent of viewing direction. The radiant flux may be emitted, transmitted, and/or reflected by the surface. Lambertian surfaces differ from any other type of surface because they reflect incident flux completely diffusely. That is to say, the distribution of radiation leaving the surface is not changed by the angle of incidence of incoming radiation [Ashdown, 2002 [60]].

Land Cover Type: The Earth's surface can be split into many categories. For example; water, shrubs, bare soil, sand, rock, snow etc. As remote sensing techniques have advanced, the number of categories has increased, and the accuracy of allocation of land type to an area has increased.

Nadir: The point on the Earth directly below the satellite.

Nadir BRDF-Adjusted Reflectance (NBAR): gives the surface reflectance from a nadir viewing position (directly above the point being viewed).

Swath (width): The width of the observed area across the track of the instrument's orbit is called the swath. The swath differs from the Across-track characteristic because it is a distance, whereas the Across-track characteristic of a satellite is an angle. The swath width in Figures 7 and 8 is the distance from one side of the viewed ground to the other (perpendicular to the track).

Track: Refers to the path on the Earth that is directly below the satellite during its orbit.

White Sky Albedo: See Bi-Hemispherical Reflectance.

Zenith Angle: Consider a point where a measurement is to be taken, (labelled 'A' in Figure 9) and another point directly above it (labelled 'B' in Figure 9). Point 'B' is called the zenith. If a satellite is looking at point 'A' from point 'C', then the (viewing) zenith angle is angle CAB. The Solar Zenith Angle is simply a special case of the zenith angle. Consider two points along a radius of the Earth; one on the Earth's surface (labelled 'A' in the Figure 9), and one further out (labelled 'B' in the Figure 9). The angle between the line AB, and the line from A to the Sun, is called the Solar Zenith Angle -the angle SAB.

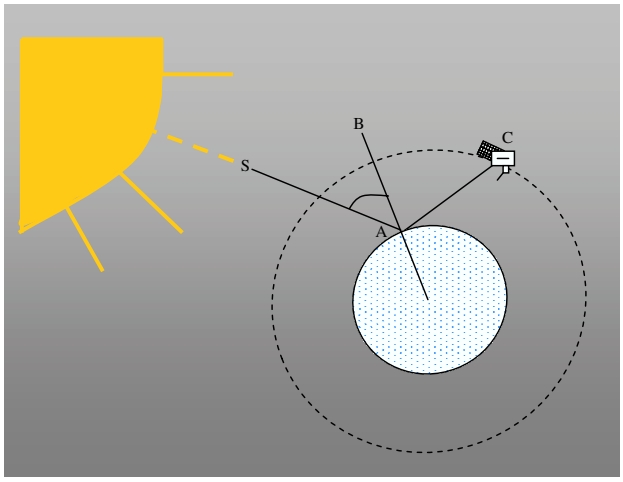

Figure 9: Zenith Angle (CAB) and Solar Zenith Angle (SAB).

B List of Acronyms

ALI Advanced Land Imager

AMBRALS Algorithm for MODIS Bidirectional Reflectance Anisotropy of the Land Surface

ASAS Advanced Solid-state Array Spectroradiometer

ASTER Advanced Spaceborne Thermal Emission and Reflection Radiometer

AATSR Advanced Along-Track Scanning Radiometer

ATSR Along-Track Scanning Radiometer

AVHRR Advanced Very High Resolution Radiometer

BOREAS BOReal Ecosystems Atmosphere Study

BRDF Bidirectional Reflectance Distribution Function

CBERS China/Brazil Earth Resources Satellite

CCD Charge-Coupled Device

CSAR Coupled Surface-Atmosphere Reflectance

DORIS Doppler Orbitography and Radiopositioning Integrated by Satellite

EOS Earth Observing System

ERBE Earth Radiation Budget Experiment

EROS Earth Remote Observation System

ETM+ Enhanced Thematic Mapper Plus

GCM General Circulation Model

HRG High Resolution Geometric

HRS High Resolution Stereoscopic

HYDROS HYDROsphere State

IGBP International Geosphere Biosphere Program

ISLSCP International Satellite Land Surface Climatology Project

LAI Leaf Area Index

MISR Multiangle Imaging SpectroRadiometer

MODIS MODerate Resolution Imaging Spectroradiometer

MVA Multiple View Angle

NASA National Aeronautics and Space Administration

NBAR Nadir BRDF-Adjusted surface Reflectances

NDVI Normalised Difference Vegetation Index

NOAA National Oceanic and Atmospheric Agency

NPOESS National Polar-orbiting Operational Environmental Satellite System

PARABOLA Portable Apparatus for Rapid Acquisition of Bidirectional Observation of the Land and Atmosphere

POLDER POLarization and Directionality of the Earth's Reflectances

RMSE Root Mean Square Error

SPOT Système Pour l'Observation de la Terre

TIROS Television InfraRed Observation Satellite

TM Thematic Mapper

References

[1] Xue, Y., and Shukla, J., The influence of land surface properties on SaheSystème Probatoire d'Observation de la Terrel climate, Part 1, Desertification, J. Clim., 6, 1993.

[2] Hahmann, A. N., and Dickinson, R. E., RCCM2/BATS model over tropical South America: Applications to tropical deforestation, J. Clim., 10, 1944-1964, 1997.

[3] Charney, J. G., Quirk, W. J., Chow, S. H., and Kornfield, J., A comparative study on the effects of albedo change on drought in semi-arid regions, J. Atmos. Sci,. 34, 1366-1385, 1977.

[4] Dickinson, R. E., and Hanson, B., Vegetation-albedo feed-backs, in Climate Processes and Climate Sensitivity, Geophys. Monogr., vol. 29, edited by J. E. Hanson and T. Takahashi, AGU, Washinton, D.C., 1984.

[5] Lucht, W., Hyman, A. H., Strahler, A. H., Barnsley, M. J., Hobson, P., and Muller, J. P., A comparison of satellite derived spectral albedos to ground-based broadband albedo measurements modeled to satellite spatial scale for a semidesert landscape, 2000.

[6] Kaicun, W., Liu, J., Zhou, X., Sparrow, M., Ma, M., Sun, Z., and Jiang, W., Validation of the MODIS global land surface albedo product, 2004.

[7] Monteith, J. L., Principles of Environmental Physics, Edward Arnold, London, 1973.

[8] Maurer, J. Retrieval of surface albedo from space, 2002.

[9] Sellers, P. J., Remote Sensing of the land surface for studies of global change. NASA/GSFC International satellite land surface climatology project report, 1993.

[10] Liang, S., Shuey, J. C., Russ, A. L., Fang, H., Chen, M., Walthall, C. L., Daughtry, C. S. T., and Hunt, Jr., R., Narrowband to broadband conversions of land surface albedo, 2003.

[11] Stroeve, J., Nolin, A., and Steffen, K., Comparison of AVHRR-derived and in situ surface albedo over the Greenland ice sheet, 1997.

[12] Nicodemus, F. E., Directional reflectance and emissivity of an opaque surface, 1965.

[13] Ni, W., and Li, X., A coupled vegetation-soil bidirectional reflectance model for a semiarid landscape, 2000.

[14] Vermote, E. F., El Saleous, N. Z., Justice, C. O., Kaufman, Y. J., Privette, J., Remer, L., Roger, J. C., and Tanr, D., Atmospheric correction of visible to middle infrared EOS-MODIS data over land surface, background, operational algorithm and validation, Journal of Geophysical, 1997.

[15] Wanner, W., and Strahler, A. H., Global retrieval of bidirectional reflectance and albedo over land from EOS MODIS and MISR data: theory and algorithm. J. Geophys. Res., 1997.

[16] Brown de Costoun, E.C., Walthall, C.L., Cialella, A.T., Vermote, E.R., Halthore, R.N., Irons, J.R., Variability of BRDF with land cover type for the west central HAPEX-Sahel super site, 1996.

[17] Sutherland, M., Barnsley, M., Lewis, P., Muller, J-P., Estimating Land Surface Albedo in the HAPEX-Sahel Southern Super-Site: Inversion of Two BRDF Models against Multiple Angle ASAS Images, 1997.

[18] Wei, X., Hahmann, A. N., Dickinson, R. E., Yang, Z. L., Zeng, X., Schaudt, K. J., Schaaf, S. B., Strugnell, N., Comparison of albedos computed by land surface models and evaluation against remotely sensed data, 2001.

[19] Barnsley, M. J., Strahler, A. H., Morris, K. P., and Muller, J. P., Sampling the surface bidirectional reflectance distribution function: Evaluation of current and future satellite sensors, 1994.

[20] Latry, C. and Roug, B., In Flight Commissioning of SPOT5 THR Quincunx Sampling Mode, 2002.

[21] Barre, L., Thomas, S., Jacob, P., Foisneau, T., Vilaire, D., and Pochard, M., Night Sky Tests and In-Flight Results of SED16 Autonomous Star Sensor, Proceedings of the 26th AAS Conference on Guidance and Control, Advances in the Astronautical Sciences, 2003.

[22] http://landsathandbook.gsfc.nasa.gov/handbook-/handbook_htmls/chapter3/chapter3.html

[23] http://landsat.gsfc.nasa.gov/about/etm+.html

[24] http://eo1.gsfc.nasa.gov/Technology/eo1Technology.html

[25] http://www.leos.le.ac.uk/aatsr/index.htm

[26] Prata, F., Land Surface Temperature Measurement from Space: AATSR Algorithm Theoretical Basis Document, 2002.

[27] Strugnell, N., and Lucht, W., Continental-scale albedo inferred from AVHRR data, land cover class and field observations of typical BRDFs, 2001.

[28] Csiszar, I., and Gutman, G., Mapping global land surface albedo from NOAA AVHRR, 1999.

[29] Greuell, W., and Oerlemans, J., Validation of AVHRR- and MODIS-derived albedos of snow and ice surfaces by means of helicopter measurements, 2005.

[30] Hautecoeur, O., and Roujean, L. J., Validation of POLDER surface BRDF and albedo products based on a review of other satellites, ground and climate databases, 2007.

[31] ASTER website: http://asterweb.jpl.nasa.gov/

[32] Tsuchida, S., Snow BRDF effects on vicarious and cross calibrations of ASTER, 1999.

[33] MODIS website: http://modis.gsfc.nasa.gov/about/

[34] Schaaf, C. B. et al., Remote Sensing of Environment 83, 2002.

[35] http://terra.nasa.gov/About/MISR/about_misr.html

[36] Diner, D. J. et al., Performance of the MISR Instrument During Its First 20 Months in Earth Orbit, 2002.

[37] Diner, D. J., Braswell, R., Davies, R., Gobron, N., Jin, Y., Kahn, R. A., Knyazikhin, Y., Loeb, Y., Muller, J. P., Nolin, A. W., Pinty, B., Schaaf, C. B., and Stroeve, J., New directions in Earth observing: Scientific applications of multiangle remote sensing, 2004.

[38] Zhang, Y. C., Rossow, W. B., and Lacis, A. A., Calculation of surface and top of atmosphere radiative fluxes from physical quantities based on ISCCP data sets, 1995.

[39] Running, S. W. et al., Terrestrial remote sensing science and algorithms planned for EOS/MODIS, 1994.

[40] Disney, M. I., Lewis, P., Thackrah, G., Quaife, T., and Barnsley, M. J., Comparison of MODIS broadband albedo with values derived from other EO data at a range of scales and ground measurements, 2004.

[41] Chen, L., Li, X., Gao, F., and Strahler, A., Derivation and validation of a new kernel for kernel-driven BRDF models, 1999

[42] Privette, J. L., and Vermote, E. F., Fitting remote sensing data with linear bidirectional reflectance models, 1995.

[43] Ross, J. K., The radiation regime and architecture of plant stands. Norwell, MA: Dr. W. Junk, [1981].

[44] Li, X., and Strahler, A. H., Geometric optical bidirectional reflectance modelling of the discrete crown vegetation canopy: effect of crown shape and mutual shadowing. IEEE Trans. Geosci. Remote Sens., 1992.

[45] Privette, J. L., Eck, T. F., and Deering, D. W. Estimating spectral albedo and nadir reflectance through inversion of simple BRDF models with AVHRR/MODIS-like data. J. Geophys. Res., 1997.

[46] Wanner, W., Li, X., and Strahler, A. H., On the derivation of kernels for kernel-driven models of bi-directional reflectance. J. Geophys. Res., 1995.

[47] Lucht, W., and Lewis, P., Theoretical noise sensitivity of BRDF and albedo retrieval from the EOS-MODIS and MISR sensors with respect to angular sampling. Int. J. Remote Sensing, 2000.

[48] Lucht, W., Expected retrieval accuracies of bidirectional reflectance and albedo from EOS-MODIS and MISR angular sampling. J. Geophys. Res., 1998.

[49] Li, Z., Cihlar, J., Zheng, X., Moreau, L., and Ly, H., The bidirectional effects of AVHRR measurements over boreal regions, 1996.

[50] Wu, A., Li, Z., and Cihlar, J., Effects of land cover type and greenness on advanced very high

resolution radiometer bidirectional reflectances: Analysis and Removal, 1995.

[51] d'Entremont, R. P., Schaaf, C. B., and Strahler, A. H., Cloud detection and land surface albedos using visible and near-infrared bidirectional reflectance distribution models, 1996.

[52] Strahler, A. H., Wanner, W., Zhu, Q., and Jin, X., Bidirectional reflectance modelling of data from vegetation obtained in the Changchun Solar Simulation Laboratory, 1995.

[53] Liang, S., Strahler, A. H., Zhu, Q., and Jin, X., Comparisons of radiative transfer models of vegetation canopies and laboratory measurements, 1997.

[54] Barnsley, M. J., Lewis, P., On the information content of Multiple View Angle (MVA) images, 1997.

[55] Deering, D. W., Ahmad, S. P., Eck, T. F., and Banerjee, B. P., Temporal attributes of the bidirectional reflectance for three boreal canopies, 1995.

[56] Flynn, L. J., Wu, W., Downs, W. R., Baoxin, H., Lucht, W., Li, X., and Strahler, A. H., Validation of kernel-driven semiempirical models for the surface bidirectional reflection distribution function of land surfaces, 1997.

[57] Stroeve, J., Box, J. E., Gao, F., Liang, S., Nolin, A., and Schaaf, C., Accuracy assessment of the MODIS 16-day albedo product, 2005.

[58] Sabins, F. F., Remote Sensing: Principles and Interpretation, 1979.

[59] Poehls, D. J., and Smith, G. J., Encyclopedic Dictionary of Hydrogeology, 2007.

[60] Ashdown, I., Radiosity: A programmer's perspective, 2002.